Received: 7 March 2017 | Revised: 6 June 2017 | Accepted: 26 June 2017

DOI: 10.1002/pip.2919

WILEY PROGRESS IN PHOTOVOLTAICS

SHORT COMMUNICATION

Highly transparent singlet fission solar cell with multistacked thin metal contacts for tandem applications

Ju Min Lee[1] | Moritz H. Futscher[1] | Luis M. Pazos-Outón[2] | Bruno Ehrler[1]

[1] Center for Nanophotonics, AMOLF, Science Park 104, 1098 XG, Amsterdam, The Netherlands

[2] Electrical Engineering and Computer Sciences Department, University of California, Berkeley, CA 94720-1770, USA

Correspondence
Bruno Ehrler, Center for Nanophotonics, AMOLF, Science Park 104, 1098 XG, Amsterdam, The Netherlands
Email: b.ehrler@amolf.nl

Abstract

Singlet fission solar cells combined with silicon photovoltaics allow the construction of parallel tandem solar cells, which benefit from better usage of high-energy photons. A key limiting factor for the performance of such a tandem configuration is the transparency of the singlet fission front cell. Here we show highly transparent singlet fission solar cells with a top contact of thin Ca:Ag blends. The optimized contact leads to 81% average solar cell transmittance in the near-infrared while maintaining more than half the short-circuit current density compared with an opaque device. We simulate the performance of the parallel tandem stack and assess the improvements needed to fully realize the potential of singlet fission in this device configuration.

KEYWORDS

singlet fission, small molecule semiconductor, solar cell, tandem solar cell, transparent electrode

Charge carrier multiplication in solar cells allows the extraction of more than one charge carrier per absorbed photon.[1] This multiplication effect increases the theoretical power conversion efficiency (PCE) limit from 34% to 45%.[2,3] One of the most promising carrier multiplication mechanisms is a process known as singlet fission, where a spin-singlet exciton, generated by the absorption of a high-energy photon, spontaneously converts into two triplet excitons with half of the original singlet exciton energy. Small molecule organic semiconductors, such as pentacene, facilitate very high singlet exciton to triplet exciton conversion yields, approaching 200%.[4-6] Thus, in configurations where these triplet excitons can be extracted, the photocurrent of the device can be increased.[7] One implementation of singlet fission-based solar cells is the use of parallel-connected tandem devices, where the singlet fission cell acts as the high-band gap front cell in conjunction with a narrow-band gap solar cell. Down-conversion via singlet fission facilitates voltage-matching between the high- and the low-band gap subcells. Recently, we demonstrated such a parallel connected tandem solar cell based on pentacene and crystalline silicon.[8] Such voltage-matched parallel connected tandem solar cells show more stable performance under a change of solar spectrum compared with the most common current matched series-connected tandem devices. However, parallel tandem solar cells did not achieve a high PCE so far due to optical losses at the front solar cell. Ideally, the front cell would absorb all photons above the band gap of the singlet fission material and be perfectly transparent at energies below that band gap to maximize the number of harvested photons in the back cell. Therefore, the performance of the tandem stack is crucially determined by the transparency of the singlet fission front cell.

Here we investigate highly transparent, inverted pentacene solar cells with two transparent contacts, an ITO bottom contact and a thin metal layer stacked top contact. The semiconducting singlet fission layer acts as a filter that absorbs high-energy photons, while being perfectly transparent to below band gap radiation. Consequently, below band gap transparency is critically limited by the near-infrared (NIR) transparency of the electrodes in such devices. Therefore, we focus on the fabrication of a conductive and transparent top metal electrode. Indium tin oxide (ITO) is the most common material used for transparent contacts because of its remarkable optical transparency and electrical conductivity.[9] However, ITO deposition demands high power sputtering, which would decompose any underlying organic layer during the deposition process. Metal nanowire networks,[10-12] nanomeshes,[13,14] and carbon nanostructures based on carbon nanotubes[15,16] and graphene[17] have shown sufficient optical transparency and electrical conductivity as a top electrode for semitransparent organic solar cells. However, those nanostructured layers are assembled by wet chemical processing and thermal annealing to form a uniform and electrically conductive layer. A predeposited organic layer can be dissolved or degraded by solvents during those processes. Recently, it was shown that multilayers of thin metals can lead to >90% of optical transparency with an electrical conductivity comparable with ITO.[18-20] This multilayer structure is easily prepared by a mild thermal evaporation process, which avoids the degradation of the

 Copyright © 2017 John Wiley & Sons, Ltd.

underlying organic layers during the deposition. Despite the advantages, multistacked metal electrodes are designed for hole-carrier collection, whereas conventional singlet fission-based solar cells require electron extraction at the top electrode.

We introduce an inverted singlet fission-based organic solar cell to incorporate the highly transparent multilayer electrode. The device architecture and energy band diagram of conventional and inverted singlet fission-based organic solar cells are illustrated in Figure 1(a) and (b). For the conventional singlet fission cell, we follow Congreve et al,[6] using a heterojunction between pentacene and C_{60} fullerene with poly(3,4-ethylenedioxythiophene) polystyrene sulfonate (PEDOT:PSS)/poly(3-hexylthiophene-2,5-diyl) (P3HT) as the hole extraction layers and bathocuproine (BCP) as the electron extraction layer. For the inverted cell, we use molybdenum oxide (MoO_x) as the hole extraction (top) layer and zinc oxide (ZnO) as the bottom electron extraction layer. The current density-voltage (*J-V*) performance of opaque conventional and inverted solar cells are shown in Figure 1(c) and summarized in the inset. The conventional cell shows a short-circuit current density (J_{SC}) of 6.7 ± 0.3 mA/cm^2, which is higher than the J_{SC} of 5.1 ± 0.2 mA/cm^2 from the inverted cell. However, the inverted solar cell shows superior open-circuit voltage (V_{OC}) of 0.40 ± 0.01 V and fill factor (FF) of 56% ± 2% in comparison with the conventional cell with a V_{OC} of 0.34 ± 0.01 V and an FF of 45 ± 1%, resulting in 1.12 ± 0.1% of average PCE.

The solar cell performance is significantly affected by the thickness of the pentacene layer. We optimized the thickness of pentacene in the inverted solar cell from 20 to 100 nm to find the ideal thickness, as shown in the *J-V* curves in Figure 1(d). J_{SC} increases with the thickness from 20 to 100 nm. The enhanced absorption of the thicker pentacene layer presumably leads to higher exciton generation rate while still allowing for most excitons to reach the pentacene/C_{60} interface. The V_{OC} of the solar cells is also increased when the pentacene thickness is increased, presumably because of voids forming in the thin pentacene films (see Supplementary Information S2). At higher thicknesses, the J_{SC} and V_{OC} drop due to recombination in the pentacene layer as the layer thickness exceeds the exciton diffusion length.[21,22] In addition, the thicker layers (≥80 nm) lead to less reproducible results, presumably because of the rougher surface morphology of the thick layers (see Supplementary Information S2). In the following, we will use solar cells with 60 nm of pentacene.

To optimize the optical transparency of the pentacene solar cell for the tandem device configuration, we introduced 2 different semi-transparent top electrodes composed of multistacked metals replacing the conventional opaque metal electrode. First, we simply reduced the

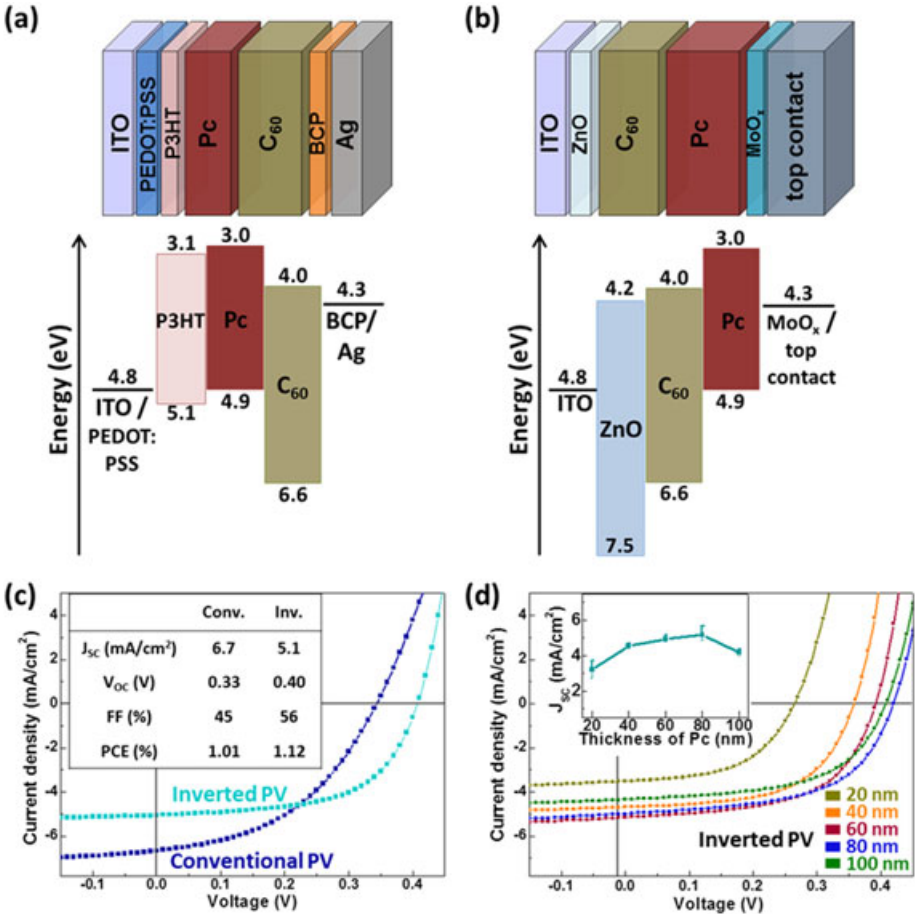

FIGURE 1 Illustration of the solar cell architecture and energy band diagram of (a) the conventional pentacene solar cell based on reference[6] and (b) the inverted solar cell with different top contact structures such as the opaque silver (100 nm thick), transparent thin silver and transparent calcium:silver blended layer. (c) Current density-voltage (*J-V*) characteristics of conventional and inverted solar cells. d, *J-V* characteristics and short-circuit current density (J_{SC}, inset) of inverted solar cells with 20 to 100 nm of pentacene layer thickness [Colour figure can be viewed at wileyonlinelibrary.com]

thickness of the Ag layer down to 10 nm. To achieve uniform Ag deposition, we deposited 1 nm of aluminum (Al) underneath of Ag as a seed layer. The transmittance of the semitransparent inverted pentacene solar cell with the thin Al/Ag contact is shown in Figure 2(a). Upon reducing the thickness of Ag from 70 to 10 nm, the transmittance in the visible to NIR region (400–1100 nm) increases from 5% to 40%. To reduce the reflection from the top electrode, we introduced 94 nm of molybdenum oxide (MoO_x) on top of the Al/Ag electrode as an antireflection (AR, λ/4 = 225 nm) coating considerably enhancing the transmittance of the device in the near-IR region (dashed lines in Figure 2(a)). Figure 2(b) shows the average transmittance of the full device in the visible region (400 to 800 nm, T_{vis}) and the region below the pentacene band gap, which we call NIR region (700 to 1100 nm, T_{NIR}) as a function of Ag layer thickness. The transmittance continuously decreases with top contact thickness. With the AR coating, both T_{NIR} and T_{vis} are enhanced by 5%–15%. The sheet resistance (R_S) of the contact has to be considered for efficient charge collection in a solar cell. Ag contacts of all thicknesses without AR coating present R_S below 6 Ω/□ except for the 10 nm Ag contact with much larger R_S of 127 Ω/□ (see Figure 2(c)), presumably because of the formation of unconnected Ag domains.[19]

The second semitransparent multilayer metal contact we apply is a blend of calcium and silver (Ca:Ag). Schubert et al. showed that this combination of materials exhibits an unusually high optical transmittance, while maintaining good conductivity.[20,23] We sequentially deposited 1 nm of Al and Ag seed layers on top of the solar cell structure to achieve a uniform Ca:Ag layer. Ca and Ag were co-evaporated to form a blend that self-assembles as a Ag network surrounded by a Ca shell.[23] Figure 2(d) shows the transmittance of semitransparent solar cells with varying Ca:Ag thicknesses. All devices with Ca:Ag electrodes show superior transmittance, almost 30% higher over the entire wavelength range in comparison with devices with the same thickness of thin Ag electrode. As an AR coating, we used 90 nm of tris(8-hydroxyquinolinato)aluminium (Alq_3) on top of the Ca:Ag electrode, following Schubert et al[23] (dashed line in Figure 2(d)). The AR coating is designed to maximize T_{NIR} (λ/4 = 200 nm) and thus decreases the T_{vis}, whereas T_{NIR} is enhanced by around 10% for all Ca:Ag thicknesses. The AR layer enhanced the transparency of the solar cell in the 700 to 1100 nm region even more significantly compared with the thin Ag electrode. The device with 10 nm of Ca:Ag electrode with AR coating achieved the maximum transmittance of 92% at 820 nm. T_{vis} and T_{NIR} are decreasing with increasing Ca:Ag layer thickness, but with a much weaker thickness dependence compared with the thin Ag electrode (Figure 2(b) and (e)). The thickness of the Ca:Ag layer also determines the electrical performance, and in the following, we optimize the solar cell for best overall performance. The MoO_x/Al/Ag/Ca:Ag structure shows higher R_S than the MoO_x/Al/thin Ag for all layer thickness (see Figure 2(f)). The 40 nm of Ca:Ag contact allows 29 Ω/□ of R_S with 60% of T_{NIR}, which is comparable with the 22 Ω/□ of our commercial ITO (125 nm), whereas it sharply increases to 140 Ω/□ at 10 nm of Ca:Ag contact, unfavorable for solar cell operation. We note that the resistance of our Ca:Ag contact is higher than reported previously for this electrode,[23] presumably because the surface roughness of the underlying active layer is larger (see Supplementary Information S2).

J-V characteristics of semitransparent solar cells with thin Ag and Ca:Ag electrodes of varying thickness are shown in Figure 3(a) and (b), respectively. A semitransparent solar cell with a thin Ag (40 nm) electrode 0.90% of PCE shows a performance of only slightly less than the opaque solar cell (Figure 3(a), full solar cell details in Supplementary Information Table S3). The solar cell performance is almost identical with and without the AR coating (Supplementary Information S4). When the Ag thickness is reduced to 20 nm to yield higher transmission (T_{NIR} of 40%), the solar cell performance is considerably reduced (PCE, 0.45%), mostly due to a lower J_{SC} of 2.5 mA/cm^2. The Ca:Ag

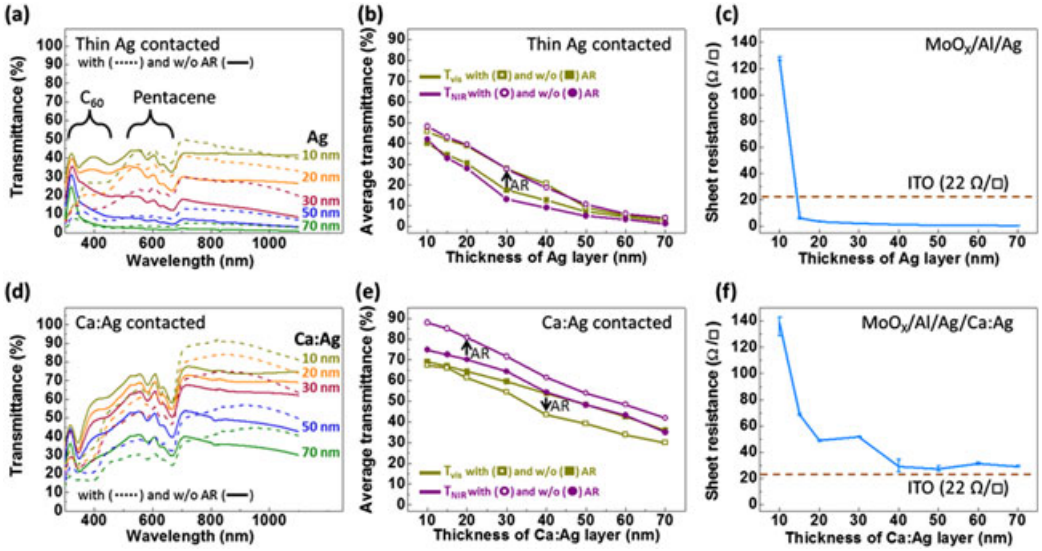

FIGURE 2 Optical transmittance of solar cell with different thickness of (a) thin Ag contact and (d) Ca:Ag contact. Brackets in panel a indicate mostly C_{60} and Pentacene absorption. Calculated average transmittance of solar cell in visible (400 to 800 nm, T_{vis}) and near infrared (700 to 1100 nm, T_{NIR}) region with (b) thin Ag contact and (e) Ca:Ag contact with and without antireflection (AR) coating. Sheet resistance as a function of layer thickness of (c) Ag and (f) Ca:Ag without AR coating. The dashed lines show the sheet resistance of our commercial ITO (125 nm) [Colour figure can be viewed at wileyonlinelibrary.com]

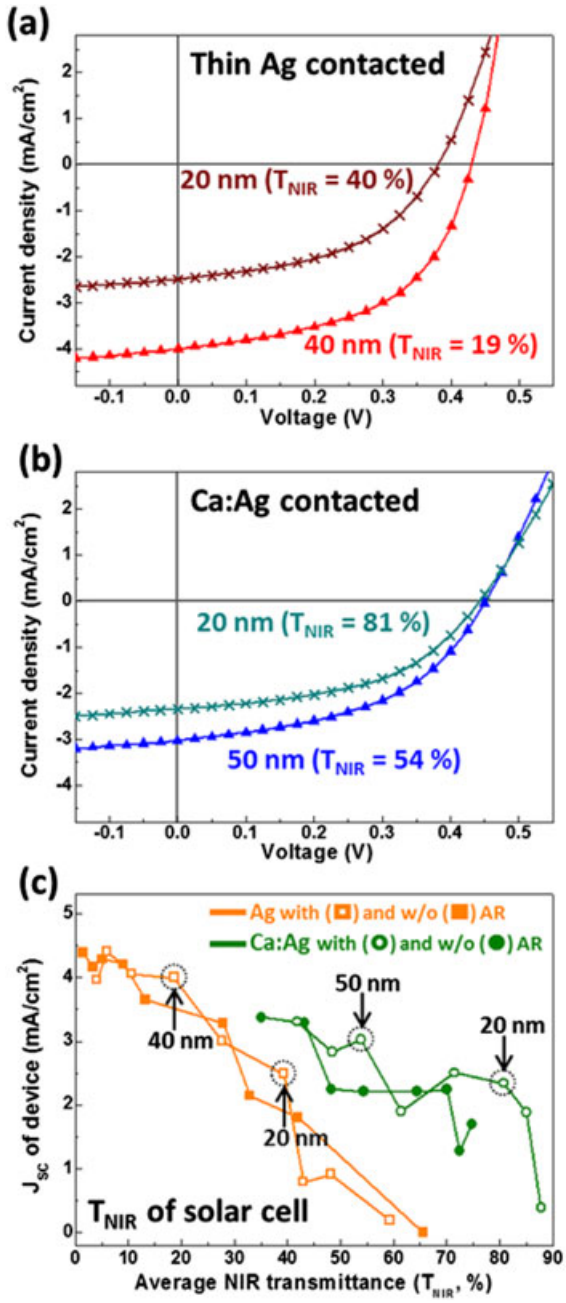

FIGURE 3 *J-V* characteristics of semitransparent solar cells with (a) thin Ag contact and (b) Ca:Ag contact. (c) J_{SC} of semitransparent solar cells with the 2 types of top contact as a function of T_{NIR} for solar cells with and without AR coating [Colour figure can be viewed at wileyonlinelibrary.com]

electrode allows for much higher T_{NIR} values for comparable solar cell efficiencies. The AR-coated semitransparent solar cell with a 50 nm thick Ca:Ag electrode presents 3.0 mA/cm^2 of J_{SC}, and a PCE to 0.64% at 54% of T_{NIR} (see Figure 3(b)). An extremely transparent solar cell with only 20 nm Ca:Ag layer shows 81% of T_{NIR} while maintaining 2.3 mA/cm^2 of J_{SC}, yielding 0.50% of PCE. We note that the reduction in J_{SC} in the transparent solar cell is mostly because of the absence of a reflective silver contact. The reflection off the silver contact allows designing the organic solar cell as a Fabry-Perot cavity, leading to much stronger absorption in the pentacene layer.[24] Transparent solar cells thus require materials with large triplet exciton diffusion length or selective reflectivity of the contact. Figure 3(c) summarizes the J_{SC} as a function of T_{NIR} with the 2 types of electrodes. The Ca:Ag layer yields nearly 20% higher T_{NIR} for the same J_{SC} value than solar cells based on the Al/Ag contact. J_{SC} continuously decreases to half the value of the opaque device at 70% of T_{NIR} owing to lower conductivity and reduced reflection off the back contact. V_{OC} and FF are almost identical for all contact thicknesses >10 nm.

Semitransparent singlet fission solar cells can be used as the front cell of a tandem device configuration in combination with a Si back cell. Singlet fission allows the connection of devices in a 2-terminal parallel cell (Figure 4(a)), ensuring higher spectral stability compared with conventional, series connected tandem cells[8] while maintaining the 2-terminal advantage compared with 4-terminal cells (Figure 4(b)). In the following, we calculate the potential singlet fission/Si tandem solar cell efficiency based on the transmittance spectrum and the performance of the semitransparent singlet fission front cells with different Ca:Ag thicknesses (see Supplementary Information S6 for details of the simulation).[25] Figure 4(c) shows the calculated J_{SC} of parallel tandems made from the singlet fission cells together with the record performing silicon solar cell.[26] A thick Ca:Ag contact enhances the J_{SC} of a semitransparent front cell by lowering the R_S. However, more serious photon absorption and reflection at the thick electrode reduces the J_{SC} of the Si back cell. The J_{SC} of the parallel tandem solar cell is maximized at 32.6 mA/cm^2 for 15 nm of Ca:Ag contact thickness (Figure 4(d)). However, the tandem solar cells do not yield performances higher than the Si bottom cell alone, even with the highly transparent front cell obtaining >80% of T_{NIR}. To achieve a tandem cell performance higher than the 2 individual subcells, the current of the front cell needs to be higher than the current loss from placing it in front of the silicon cell. In the final device configuration, the silicon and the singlet fission cell might share a common ITO contact. Some silicon cells already feature ITO contacts,[27] and the singlet fission cell could simply be placed on top. The AR coating of the Si cell would then need to be placed on top of the singlet fission cell. Thus, the absorption at the active layer of the singlet fission front cell needs to be maximized to benefit from carrier multiplication, while maintaining above unity quantum efficiency. In addition, the parallel tandem solar cell shows lower PCE in comparison with the 4-terminal tandem because of the large voltage difference between the maximum power point (V_{mpp}) of the semitransparent pentacene device and the Si solar cell (see Supplementary Information Figure S6). V_{mpp} matching is required in order to maximize the performance of parallel connected tandem solar cells. For this reason, singlet fission cells based on materials with a higher triplet energy (such as tetracene), and thus larger voltage, would greatly benefit the tandem solar cell performance. However, in our hands, as well as in the literature, tetracene-based singlet fission solar cells have shown lower quantum efficiency than pentacene cells,[28] despite the quantitative singlet fission in tetracene under optimized conditions.[29-31] This illustrates the requirement for optimizing device architecture, interfaces, and tetracene growth. Furthermore, the series resistance of the singlet fission solar cell is high in comparison with the Si solar cell, which degrades the FF of the parallel tandem (see Supplementary Information S2).

In summary, we have demonstrated semitransparent pentacene solar cells introducing a highly transparent top contact, which could

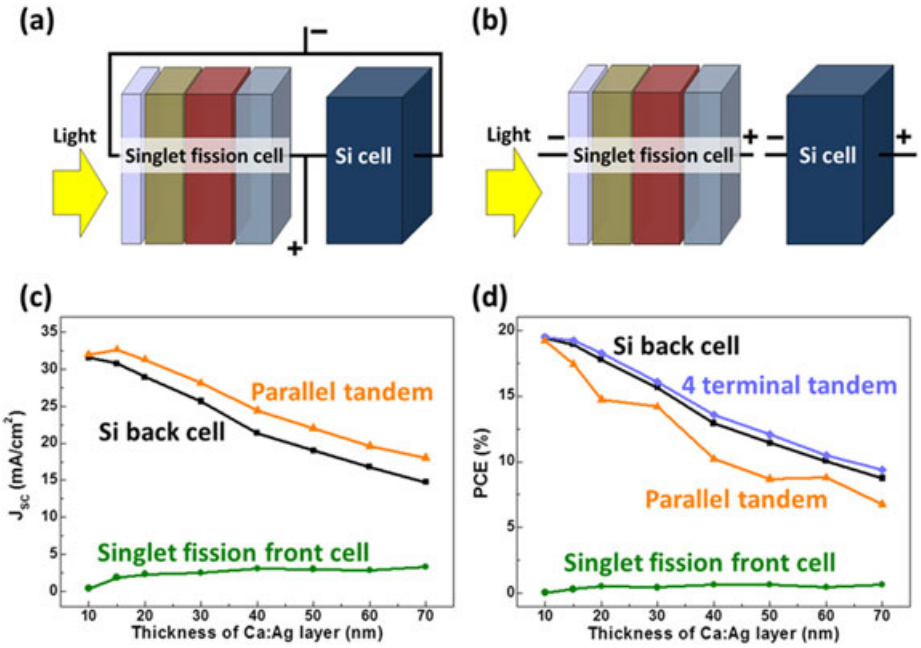

FIGURE 4 Illustration of tandem configuration based on semitransparent singlet fission front and silicon back cells. Subcells are electrically connected in (a) parallel and (b) 4-terminal. (c) Calculated J_{SC}. (d) PCE of singlet fission/Si tandem solar cells from our transparent pentacene cells with different Ca:Ag layer thicknesses [Colour figure can be viewed at wileyonlinelibrary.com]

be used to sensitize a silicon solar cell or other low-band gap cells in a parallel tandem configuration. We introduce an inverted singlet fission solar cell architecture, designed to allow for the transparent electrode, which achieves 1.21% of PCE, higher than 1.03% of conventional, non-inverted singlet fission solar cells. We characterize the inverted solar cells with thin Al/Ag and Al/Ag/Ca:Ag multistacked metals as a transparent electrode with various electrode thicknesses. Thin Ag shows low sheet resistance (below 6 Ω/□), whereas the Ca:Ag blend layer leads to a high optical transparency of the solar cell (eg, 61% of T_{NIR} with 29 Ω/□ sheet resistance at 40nm thickness). Furthermore, deposition of an antireflection layer on Ca:Ag enhanced the T_{NIR} of the solar cell. The *J-V* characteristics of semitransparent solar cells were mainly determined by the thickness of the transparent top contact. In particular, the cell with a 20-nm Ca:Ag contact showed more than half the J_{SC} of the opaque solar cell, with 81% T_{NIR}. Finally, we calculate the efficiency of a parallel tandem configuration consisting of our semitransparent singlet fission front cells together with a Si back cell, absorbing high- and low-energy photons, respectively. The compromise between transmittance and performance of the front cell determined the J_{SC} of the tandem configuration, resulting in a maximum J_{SC} of 32.6 mA/cm^2. However, reaching a higher tandem performance than the Si cell alone is still challenging using the current semitransparent singlet fission front cells. Enhancing the absorption in the active layer is critical to maximize carrier multiplication, especially for singlet fission materials with high triplet energy to improve the V_{OC} of the singlet fission cell and the overall tandem performance.

ACKNOWLEDGEMENT

The authors acknowledge Marc Duursma for his technical support and Eric Johlin for his comments on the manuscript. This work is part of the research program of The Netherlands Organization for Scientific Research (NWO).

Supporting information available: We provide details about fabrication and characterization of the semitransparent singlet fission solar cells and the model used to simulate the performance of singlet fission/Si tandem solar cells.

REFERENCES

1. Werner JH, Kolodinski S, Queisser HJ. Novel optimization principles and efficiency limits for semiconductor solar cells. *Phys Rev Lett*. 1994;72:3851-3854. https://doi.org/10.1103/PhysRevLett.72.3851
2. Shockley W, Queisser HJ. Detailed balance limit of efficiency of p-n junction solar cells. *J Appl Phys*. 1961;32:510-519. https://doi.org/10.1063/1.1736034
3. Hanna MC, Nozik AJ. Solar conversion efficiency of photovoltaic and photoelectrolysis cells with carrier multiplication absorbers. *J Appl Phys*. 2006;100:74510. https://doi.org/10.1063/1.2356795
4. Smith MB, Michl J. Singlet fission. *Chem Rev*. 2010;110:6891-6936. https://doi.org/10.1021/cr1002613
5. Rao A, Wilson MWB, Hodgkiss JM, Albert-Seifried S, Bässler H, Friend RH. Exciton fission and charge generation via triplet excitons in pentacene/C60 bilayers. *J Am Chem Soc*. 2010;132:12698-12703. https://doi.org/10.1021/ja1042462
6. Congreve DN, Lee J, Thompson NJ, et al. External quantum efficiency above 100% in a singlet-Exciton-fission–based organic photovoltaic cell. *Science*. 2013;340:334-337. https://doi.org/10.1126/science.1232994
7. Ehrler B, Walker BJ, Böhm ML, et al. In situ measurement of exciton energy in hybrid singlet-fission solar cells. *Nat Commun*. 2012;3:1019. https://doi.org/10.1038/ncomms2012
8. Pazos Outón LM, Lee JM, Futscher MH, et al. A silicon-singlet fission tandem solar cell exceeding 100% external quantum efficiency with high spectral stability. *ACS Energy Lett*. 2017;2:476-480. https://doi.org/10.1021/acsenergylett.6b00678
9. Bush KA, Bailie CD, Chen Y, et al. Thermal and environmental stability of semi-transparent perovskite solar cells for tandems enabled by a solution-processed nanoparticle buffer layer and sputtered ITO electrode. *Adv Mater*. 2016;28:3937-3943. https://doi.org/10.1002/adma.201505279

10. Hu L, Kim HS, Lee JY, Peumans P, Cui Y. Scalable coating and properties of transparent, flexible, silver nanowire electrodes. *ACS Nano*. 2010;4:2955-2963. https://doi.org/10.1021/nn1005232

11. Chen CC, Dou L, Zhu R, et al. Visibly transparent polymer solar cells produced by solution processing. *ACS Nano*. 2012;6:7185-7190. https://doi.org/10.1021/nn3029327

12. Bailie CD, Christoforo MG, Mailoa JP, et al. Semi-transparent perovskite solar cells for tandems with silicon and CIGS. *Energ Environ Sci*. 2015;8:956-963. https://doi.org/10.1039/C4EE03322A

13. Bryant D, Greenwood P, Troughton J, et al. A transparent conductive adhesive laminate electrode for high-efficiency organic-inorganic lead halide perovskite solar cells. *Adv Mater*. 2014;26:7499-7504. https://doi.org/10.1002/adma.201403939

14. Sciacca B, Van De Groep J, Polman A, Garnett EC. Solution-grown silver nanowire ordered arrays as transparent electrodes. *Adv Mater*. 2016;28:905-909. https://doi.org/10.1002/adma.201504045

15. Ago H, Petritsch K, Shaffer MSP, Windle AH, Friend RH. Composites of carbon nanotubes and conjugated polymers for photovoltaic devices. *Adv Mater*. 1999;11:1281-1285. https://doi.org/10.1002/(SICI)1521-4095(199910)11:15<1281::AID-ADMA1281>3.0.CO;2-6

16. Kim YH, Müller-Meskamp L, Zakhidov AA, et al. Semi-transparent small molecule organic solar cells with laminated free-standing carbon nanotube top electrodes. *Sol Energy Mater Sol Cells*. 2012;96:244-250. https://doi.org/10.1016/j.solmat.2011.10.001

17. You P, Liu Z, Tai Q, Liu S, Yan F. Efficient semitransparent Perovskite solar cells with graphene electrodes. *Adv Mater*. 2015;27:3632-3638. https://doi.org/10.1002/adma.201501145

18. Kim H, Kim HS, Ha J, Park NG, Yoo S. Empowering semi-transparent solar cells with thermal-mirror functionality. *Adv Energy Mater*. 2016;6:1-9. https://doi.org/10.1002/aenm.201502466

19. Schubert S, Meiss J, Müller-Meskamp L, Leo K. Improvement of transparent metal top electrodes for organic solar cells by introducing a high surface energy seed layer. *Adv Energy Mater*. 2013;3:438-443. https://doi.org/10.1002/aenm.201200903

20. Meiss J, Ziehlke H, Schubert S, Leo K, Riede M. Coevaporated calcium-silver metal alloys as contact for highly transparent organic solar cells. *Energy Sci Eng*. 2014;2:77-85. https://doi.org/10.1002/ese3.34

21. Yoo S, Domercq B, Kippelen B. Efficient thin-film organic solar cells based on pentacene/C 60 heterojunctions. *Appl Phys Lett*. 2004;85:5427-5429. https://doi.org/10.1063/1.1829777

22. Tabachnyk M, Ehrler B, Bayliss S, Friend RH, Greenham NC. Triplet diffusion in singlet exciton fission sensitized pentacene solar cells. *Appl Phys Lett*. 2013;103:4-8. https://doi.org/10.1063/1.4824420

23. Schubert S, Müller-Meskamp L, Leo K. Unusually high optical transmission in Ca:Ag blend films: high-performance top electrodes for efficient organic solar cells. *Adv Funct Mater*. 2014;24:6668-6676. https://doi.org/10.1002/adfm.201401854

24. Günes S, Neugebauer H, Sariciftci NS. Conjugated polymer-based organic solar cells. *Chem Rev*. 2007;107:1324-1338. https://doi.org/10.1021/cr050149z

25. Futscher MH, Ehrler B. Efficiency limit of perovskite/Si tandem solar cells. *ACS Energy Lett*. 2016;1:863-868. https://doi.org/10.1021/acsenergylett.6b00405

26. Green MA, Emery K, Hishikawa Y, et al. Solar cell efficiency tables (version 49). *Prog Photovoltaics Res Appl*. 2017;25:3-13. https://doi.org/10.1002/pip.2855

27. Knight MW, van de Groep J, Bronsveld PCP, Sinke WC, Polman A. Soft imprinted Ag nanowire hybrid electrodes on silicon heterojunction solar cells. *Nano Energy*. 2016;30:398-406. https://doi.org/doi.org/10.1016/j.nanoen.2016.10.011

28. Wu TC, Thompson NJ, Congreve DN, et al. Singlet fission efficiency in tetracene-based organic solar cells. *Appl Phys Lett*. 2014;104:193901 https://doi.org/10.1063/1.4876600

29. Burdett JJ, Bardeen CJ. Quantum beats in crystalline tetracene delayed fluorescence due to triplet pair coherences produced by direct singlet fission. *J Am Chem Soc*. 2012;134:8597-8607. https://doi.org/10.1021/ja301683w

30. Tayebjee MJY, Clady RGCR, Schmidt TW. The exciton dynamics in tetracene thin films. *Phys Chem Chem Phys*. 2013;15:14797-14805. https://doi.org/10.1039/C3CP52609G

31. Piland GB, Bardeen CJ. How morphology affects singlet fission in crystalline tetracene. *J Phys Chem Lett*. 2015;6:1841-1846. https://doi.org/10.1021/acs.jpclett.5b00569

SUPPORTING INFORMATION

Additional Supporting Information may be found online in the supporting information tab for this article.

How to cite this article: Lee JM, Futscher MH, Pazos-Outón LM, Ehrler B. Highly transparent singlet fission solar cell with multistacked thin metal contacts for tandem applications. *Prog Photovolt Res Appl*. 2017;1–6. https://doi.org/10.1002/pip.2919